Rain splash transport and the law of large numbers

David Jon Furbish

Department of Earth and Environmental Sciences, Vanderbilt University, Nashville, Tennessee, USA

1 Initial thoughts

It seems we have settled on the idea that one-dimensional sediment transport by rain splash in the absence of surface flow can be described as

$$q_x = -k_1 S_x \,, \tag{1}$$

where q_x [L^2 T^{-1}] is the vertically integrated volumetric particle flux parallel to x, $S_x = \partial\zeta/\partial x$ is the slope of the land-surface elevation ζ [L] and k_1 [L^2 T^{-1}] is a coefficient that represents fluid and granular physics occurring at the raindrop and particle ballistic scales. This coefficient also represents information about the occurrence and intensity of rainfall (Furbish et al., 2009; Dunne et al., 2010, 2016). The expression (1) is deterministic, Eulerian, local and continuum-like. Alternatively we can write an entrainment form of the flux as

$$q_x = -k_2 E S_x \,, \tag{2}$$

where E [L T^{-1}] is the volumetric particle entrainment rate and k_2 [L] is a coefficient that relates the ensemble averaged particle displacement during drop impacts to the local land-surface slope. Now E represents information about the occurrence and intensity of rainfall together with the physics of entrainment, and k_2 represents only fluid and granular physics of particle motions. The expression (2) likewise is Eulerian, local and continuum-like, although it emerges from a probabilistic nonlocal description of Lagrangian particle motions (Furbish et al., 2017).

Note that (1) and (2) pertain to statistically uniform rainfall, that is, complete spatial randomness in drop impact locations. In the presence of nonuniform rainfall, for example, (2) must include an additional term involving the gradient $\partial E/\partial x$. In addition, these expressions represent the outcome of the average particle motion in relation to surface slope; they do not describe particle diffusion.

Rain splash transport occurs under highly rarefied conditions. On average, only about one particle is in motion per square centimeter at any instant during a heavy rainstorm (Furbish et al., 2017). For comparison, there are about 10^{19} molecules in a cubic centimeter of air at ordinary pressure and temperature conditions. This means that (1) and (2), although written as continuously differentiable functions, cannot be interpreted as representing continuum conditions or behavior. The flux cannot be simply expressed as the product of the mean particle velocity and the particle concentration, as with a fluid continuum. Indeed, the radial particle motions about drop impacts, aside from their parabolic trajectories,[1] are markedly different from particle motions in a continuum, notably in that they rarely interact with each other following the brief granular deformation that initially occurs during the drop impact.

Rain splash transport is special in that the excitation of particle motions is entirely external and independent of the geometrical configuration of the surface and the particles in motion, unlike processes such as aeolian sand transport and bed load transport in rivers. Moreover, the simple linear form of (1) and (2) in principle appears to hold no surprises. Stated another way,

[1] The mean free path of air molecules at ordinary pressure and temperature conditions is about 10^{-7} m. Trajectories between collisions are well approximated as straight lines. But in the rarefied (non-continuum) conditions of the outer atmosphere, these trajectories are decidedly parabolic in Earth's gravitational field.

rain splash transport is perhaps the "tamest" surface transport process imaginable. It is therefore an ideal example to examine the probabilistic elements of a deterministic (continuum-like) description of a process that is fundamentally noise driven, where rarefied conditions yield an uncertainty that is part of understanding how rain splash transport works.

The purpose of this essay therefore is to provide an explanation of how particle motions at the space and time scales of individual drop impacts are connected with the expressions (1) and (2). This explanation is not concerned with the mechanics of motion, but rather, it is centered on the probabilistic ingredients of these expressions. The interpretation of the flux emerges from consideration of the law of large numbers, but not in the conventional manner associated with particle motions and fluxes occurring in continuum conditions. The analysis clarifies the combination of time averaging and spatial resolution represented by the flux for a specified uncertainty in its magnitude.

2 Raindrop impacts and particle entrainment

Consider an inclined planar surface. The x axis is parallel to the surface and positive in the downslope direction. The horizontal y axis is parallel to the elevation contours of the surface. We now choose an area $A = XY$ with edge lengths X and Y parallel to x and y. Let I denote the raindrop impact rate, that is, the number of impacts per unit area per unit time. This rate is on the order of 10^3 m^{-2} s^{-1} in heavy rainstorms (Smith et al., 2009). Within an area A, impacts are almost certainly a Poisson process in time. The expected number of impacts within A during an interval of time T is $\mu_\mathrm{I} = IAT$ and the variance is $\sigma_\mathrm{I}^2 = IAT$. Thus the variance of the number of impacts increases indefinitely with time. We can form a coefficient of variation v_A as

$$v_A = \frac{\sqrt{\sigma_\mathrm{I}^2}}{\mu_\mathrm{I}} = \frac{1}{\sqrt{IAT}}\,, \tag{3}$$

which is a measure of the relative variability about the expected value. Note that this converges at the same rate as a so-called standard error of the estimate of the mean.

One consequence of the complete spatial randomness of the raindrop impacts is that the "filling" of an area A by impacts may require a significant interval of time, and there is a finite probability that an area will not be entirely filled even after long time. This means that there is an inherent spatial noisiness, or patchiness, in the entrainment of particles from the surface. This patchiness not only occurs from one instant to the next in relation to the spacing of the drops, it also exists in relation to the randomness of impact locations following a great number of impacts (Figure 1). The characteristic impact spacing is $l = \sqrt{1/IT}$, which converges to zero as $T^{-1/2}$ for a steady impact rate I. For the example in Figure 1, the values of l indicate that

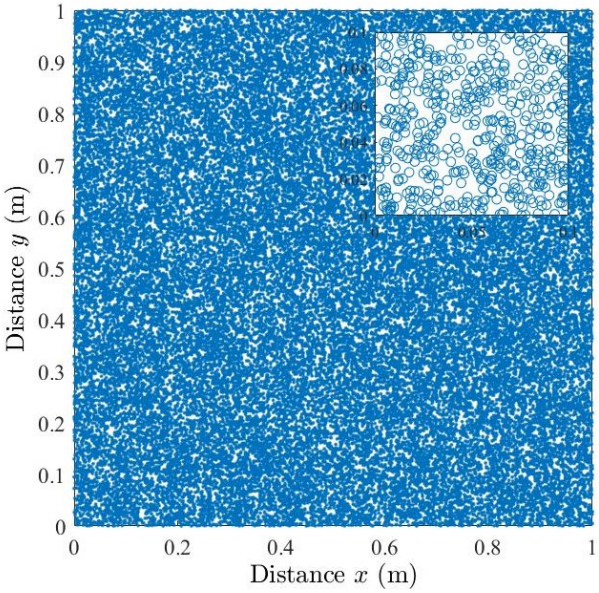

Figure 1: Plot of locations of 50 000 drop impacts within one square meter ($l \approx 0.004$ m) showing inherent patchiness of these locations. Inset is 10 cm × 10 cm. This represents 50 seconds of heavy rainfall. The plot does not become visually filled at this resolution until after about 300 000 impacts ($l \approx 0.002$ m), or about five minutes of heavy rainfall, yet patchiness in the impact locations persists.

the patchiness has a scale on the order of the diameter of typical raindrops capable of entraining particles. These points simply illustrate that because impact locations are inherently patchy, particle entrainment also is patchy rather than appearing as a smooth continuum-like quantity.

Below we are interested in the one-dimensional expression of this patchiness parallel to the downslope x coordinate. Let $f_x(x)$ denote the ensemble distribution of impact locations x within the area $A = XY$, and let $F_x(x)$ denote the cumulative distribution function. Complete spatial randomness means that the locations x are a spatial Poisson process such that $f_x(x) = 1/X$ is a uniform distribution with $F_x(x) = x/X$. For a given impact rate I and time interval T, non-overlapping intervals Δx are independent. The expected number of impacts within Δx is $IY\Delta xT$ and the variance is $IY\Delta xT$. Thus, whereas the variance in the number of impacts decreases as Δx decreases, the variability relative to the expected value, $v_{\Delta x} = 1/\sqrt{IY\Delta xT}$, increases. This means that the distribution functions $f_x(x)$ and $F_x(x)$ become smoother with increasing impact rate I and time T (Figure 2), but these converge to the continuously differentiable ensemble forms only in the limit of $T \to \infty$. For reference below, also note that this rate of convergence decreases with decreasing transverse length Y (Figure 3). For any realization, we must accept that drop impacts, and thus the entrainment rate, are patchy discontinuous quantities.

Particle entrainment varies with drop momentum (or kinetic energy) and with soil material properties and moisture content. Drop momentum and the number of entrained particles per drop are both random variables. For dry medium sand, about 10^2 particles are entrained per drop. Whereas drop impacts are Poisson in time and their locations are Poisson in space, neither the number of entrained particles nor their locations are Poisson. The locations of particle entrainment are localized at the impact crater scale; we can envision these locations as being represented by narrow distributions centered on impacts, extending outward to a distance on the order of an impact crater diameter. The distribution of

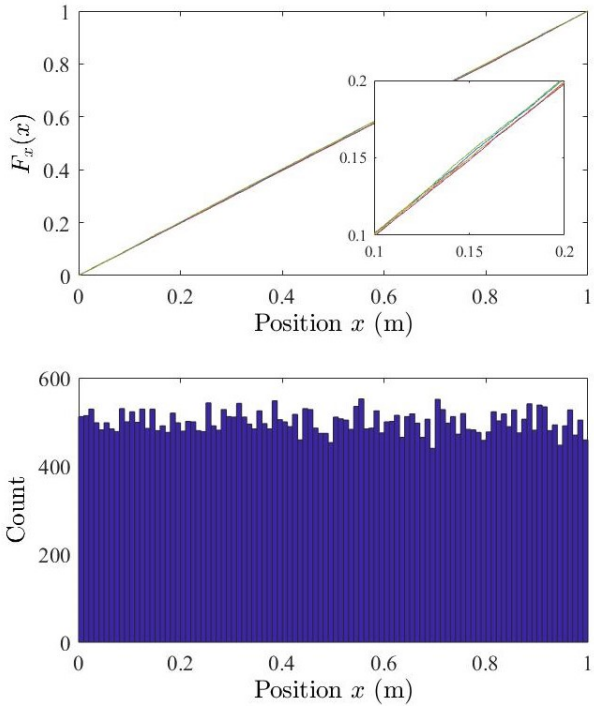

Figure 2: Plot of five realizations of cumulative distribution $F_x(x)$ for 50 000 drop impact locations x with $Y = 1$ m and histogram of one realization of locations x at 1 cm resolution.

the locations x of particle entrainment for many impacts is thus formed by superposition of the many individual, localized distributions. Then, with statistically uniform rainfall the ensemble distribution of particle entrainment locations x also is uniform. Letting n_d denote the expected number of particles entrained per drop, then the expected number entrainment rate $E_n = In_\mathrm{d}$ is uniform. The small added noise of distributing particle entrainment locations about impact centers together with the increase in numbers per impact in general leads to a distribution of entrainment locations x (Figure 4) that is smoother than the distribution of impact locations (Figure 3). Nonetheless, like the distribution of impact locations the entrainment rate E_n in any realization is a patchy discontinuous function whose irregularity increases with decreasing impact rate I, time interval T and transverse length Y. We now turn to the second part of the problem, which is centered on the distribution of particle displacements.

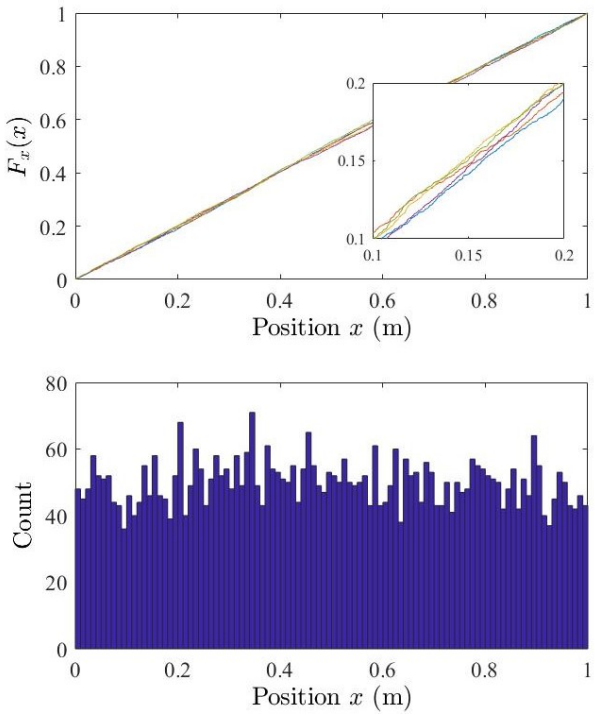

Figure 3: Plot of five realizations of cumulative distribution $F_x(x)$ for 5 000 drop impact locations x with $Y = 0.1$ m and histogram of one realization of locations x at 1 cm resolution.

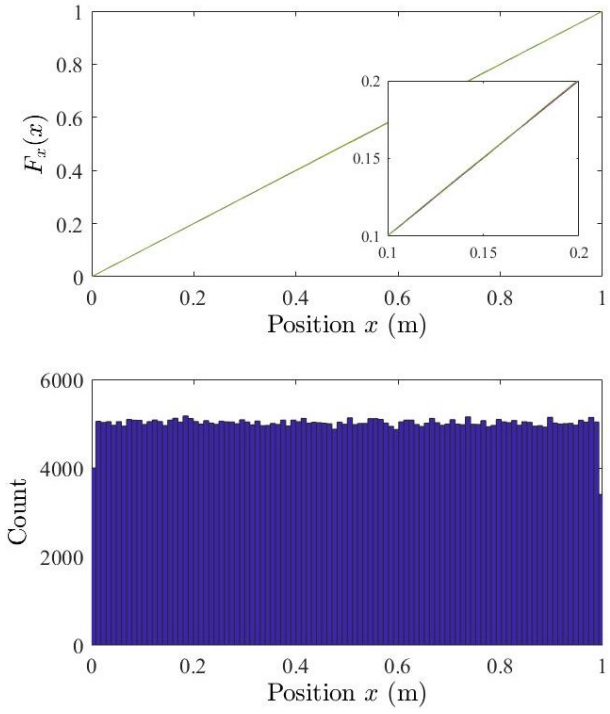

Figure 4: Plot of five realizations of cumulative distribution $F_x(x)$ for 500 000 particle entrainment locations x with $Y = 0.1$ m and histogram of one realization of locations x at 1 cm resolution. These involve 5 000 drop impacts with $n_{\rm d} = 100$.

3 Particle motions and averaging

3.1 The particle flux

Consider a line of transverse length Y positioned at x. Particles in the vicinity of this line are splashed radially about impacts in all directions. But because the surface is inclined, on average more particles are splashed in a downslope direction than in an upslope direction, and downslope displacements are longer than upslope displacements. As a consequence some particles move downslope across the line at x and some move upslope across this line. We then wish to know the difference in the number of particles that move downslope versus upslope across x during a specified interval of time T, that is, the net downslope transport.

Let $f_r(r)$ denote the ensemble distribution of particle displacements r measured parallel to x about a drop impact for specified surface slope S_x measured at a scale significantly larger than an impact crater. Assuming the first and second moments of $f_r(r)$ are defined, it is possible to show (Appendix A) that the expected net number of particles crossing x during the interval T is

$$n(T) = E_n Y \mu_r T \,, \tag{4}$$

where μ_r is the ensemble average displacement. The uncertainty in the number $n(T)$ is described in Appendix B. In turn we assume at lowest order that $\mu_r = -k_2 S_x$ (Furbish et al., 2007) which leads to

$$n(T) = -k_2 E_n Y T S_x \,. \tag{5}$$

Multiplying (5) by the individual particle volume and dividing by Y and T then leads to our starting point,

$$q_x = -k_2 E S_x \,. \tag{6}$$

It immediately follows that for an individual realization the flux q_x must be interpreted as a time averaged quantity that is implicitly associated with an unspecified averaging interval T and an unspecified transverse distance Y. Our next task is to make these quantities explicit.

3.2 Appealing to large numbers

Experiments indicate that the distribution $f_r(r)$ is a "Batman" distribution (Furbish et al., 2007) which, neglecting its "ears," can be well approximated by an asymmetric Laplace distribution with mean μ_r and variance σ_r^2 (Appendix C). Of interest is the time required to "populate" this distribution such that the initially irregular histogram of particle displacements r at small times converges to a smooth form of the distribution $f_r(r)$, which in turn implies convergence of the statistical moments to the true parametric values. Strictly speaking, this convergence requires the time interval $T \to \infty$, so in practice this is not a mathematics problem. Rather, this involves the practical matter of defining an acceptable uncertainty associated with the approximation of the mean μ_r as this depends on the averaging time T and the transverse length Y for specified impact rate I.

For this purpose we turn to the law of large numbers and the central limit theorem, which tells us that the variance $\sigma_{\overline{r}}^2$ of the estimate $\overline{r}$ of the mean μ_r is $\sigma_{\overline{r}}^2 = \sigma_r^2/N$. We may interpret the so-called standard error $\sigma_{\overline{r}}$ as a measure of the noise, or uncertainty, of the estimate $\overline{r}$ as it converges to the mean μ_r with an increasing total number N of entrained particles that populate the distribution $f_r(r)$. We now rewrite this as

$$N = \frac{\sigma_r^2}{\sigma_{\overline{r}}^2}\,, \tag{7}$$

which provides an estimate of the number of entrained particles required to consistently achieve an uncertainty specified by $\sigma_{\overline{r}}$. Note that this represents an absolute uncertainty, regardless of the mean μ_r. Further note that this uncertainty pertains to an ensemble of realizations, not an individual realization.

It is possible to show (Appendix D) that $N \approx YIn_{\mathrm{d}}\mu_{r+}T$, where μ_{r+} is the average positive displacement of entrained particles. Then (7) may be rewritten as

$$YT \approx \frac{\sigma_r^2}{In_{\mathrm{d}}\mu_{r+}\sigma_{\overline{r}}^2}\,, \tag{8}$$

This provides an estimate of the transverse length Y and the averaging interval T that are associated with the specified uncertainty represented by $\sigma_{\overline{r}}$. In particular, for a specified uncertainty an increasing averaging time T provides an estimate of the flux with increasing resolution (decreasing Y), and a decreasing averaging time leads to loss of spatial resolution.

3.3 Specifying uncertainty

For context regarding the uncertainty in rain splash transport, consider the one-dimensional form of Fick's law (Fick, 1855) for the diffusion of particles (molecules) dissolved within a liquid:

$$q_c = -k\frac{\partial c}{\partial x}\,. \tag{9}$$

Here, q_c is the mass flux parallel to x, c is the particle concentration and k is a mass diffusion coefficient. Although this local expression is deterministic, it has a rigorous probabilistic basis in kinetic theory and statistical mechanics. We use it with confidence in any realization without reference to time averaging or spatial resolution at the continuum scale, and we interpret it as an instantaneous flux without uncertainty.[2] Typically the number of particles involved is so large that averaging over the random-walk particle motions gives a precise description of the flux when measured at time scales much greater than the mean free time. We are justified in assuming the continuum hypothesis is satisfied, and we thus treat (9) as a continuously differentiable function.

This situation does not exist with the rarefied conditions of rain splash transport. One might

[2] Fick's law is actually a local approximation of nonlocal transport viewed at the molecular scale. Here, "without uncertainty" means that this approximation is more precise than our ability to detect error.

imagine that 10^5 particles entrained in a square meter during one second is a big number. Compared with continuum conditions, however, it is not; this is a tiny number. Rather than considering the particle flux q_x as representing a continuum-like quantity with negligible error, we must instead accept that it involves measurable uncertainty at short time scales. It cannot be viewed as a continuously differentiable function in any individual realization.

The average positive displacement μ_{r+} typically is on the order of centimeters. Suppose that we consider convergence of this value to within an error of 1% to be an acceptable criterion for viewing the flux as a — for lack of a better word — "quasi-continuum-like" quantity. This gives $\sigma_{\overline{r}} = 0.01$ cm, which in turn determines the combination of the transverse length Y and the averaging time T associated with this criterion. Increasing the acceptable error decreases the length Y or time T, or both; and decreasing the error increases the length Y or time T, or both. To be clear, this criterion is not aimed at prescribing the precision of the calculated flux. Rather, it is aimed at defining an uncertainty for which the flux q_x becomes sufficiently "smooth" in time that we may imagine it to be a quasi-continuous function, albeit not continuously differentiable in a strict sense. We now consider examples to illustrate these points.

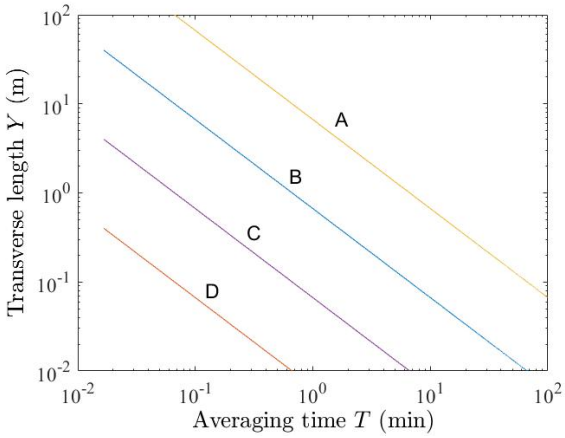

Figure 5: Plot of the transverse length Y versus the averaging time T based on number of entrained particles per impact $n_\mathrm{d} = 100$, average positive displacement $\mu_{r+} = 0.02$ m and variance $\sigma_r^2 = 2\mu_{r+}^2$ for drop impact rates and uncertainties: (A) $I = 100$ m^{-1} s^{-1} and $\sigma_{\overline{r}} = 1\%$, (B) $I = 1\,000$ m^{-2} s^{-1} and $\sigma_{\overline{r}} = 1\%$, (C) $I = 100$ m^{-2} s^{-1} and $\sigma_{\overline{r}} = 10\%$, (D) $I = 1\,000$ m^{-2} s^{-1} and $\sigma_{\overline{r}} = 10\%$.

4 Examples

Here we plot the transverse length Y versus the averaging time T for two drop impact rates I and two values of uncertainty $\sigma_{\overline{r}}$ for a fixed number of entrained particles per impact n_d and mean positive displacement μ_{r+} (Figure 5). Recall that an impact rate $I = 1\,000$ m^{-2} s^{-1} represents heavy rainfall. In general the transverse length Y decreases with increasing impact rate I and with increasing uncertainty $\sigma_{\overline{r}}$.

The transverse length Y may be interpreted as the resolution of the calculated flux necessary to achieve the specified uncertainty. For example, with heavy rainfall the resolution Y is about 1 m with an averaging time T of about 1 minute with a 1% uncertainty. To achieve a resolution of $Y = 0.1$ requires an averaging time T of about 10 minutes. These values increase by an order of magnitude with a moderate intensity rainfall, and they decrease by two orders of magnitude with a 10% uncertainty. Achieving finer resolution (smaller Y) requires a longer averaging time or increasing uncertainty, or both. A resolution that is finer than the scale at which the slope S_x is defined is not physically meaningful.

We can examine this outcome more directly. Consider a simulated realization of the number of particles crossing a position x downslope for a modest impact rate I resolved at $Y = 0.1$ m (Figure 6). Large values of $n(t)$ are associated with impacts near x and small values are associated with impacts farther upslope from x. The sequence of impacts is a Poisson process. The average particle number is initially noisy then begins to converge to the expected value with increasing averaging time T, although the rate of convergence decreases. This represents a typical realization.

In addition we plot the average particle num-

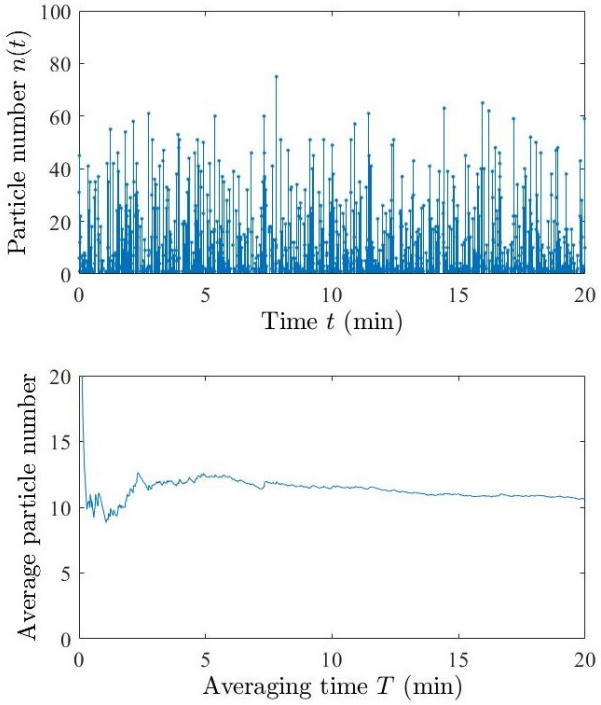

Figure 6: Plot of an individual realization of (top) the discrete number $n(t)$ of particles crossing a position x downslope and (bottom) the average number of particles crossing x with increasing averaging time T. The simulation uses $I = 100$ m^{-2} s^{-1}, $Y = 0.1$ m and $\mu_{r+} = 0.02$ m with $p_+ = 1/2$.

ber crossing x based on (18) in Appendix A for ten realizations (Figure 7). Consistent with the realization in Figure 6, the average number is initially noisy then begins to converge to the expected value with increasing averaging time T. The rate of convergence is relatively slow, which in part is attributable to the Poisson process of drop impacts. Deviations in the realizations about the expected value at large times T reflect persistence in the ensemble error. Recall that the 1% error lines in this figure are not an expected precision of the calculated flux, but rather they represent an example of a possible prescribed uncertainty for which the flux becomes sufficiently smooth in time that we may imagine it to be a quasi-continuous quantity.

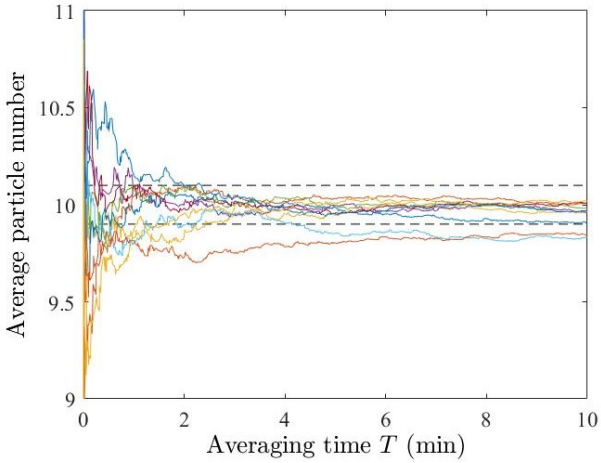

Figure 7: Plot of ten realizations of the average number of particles crossing x with increasing averaging time T. The simulation uses $I = 100$ m^{-2} s^{-1}, $Y = 0.1$ m and $\mu_{r+} = 0.02$ m with $p_+ = 1/2$ based on (18) in Appendix A. Horizontal dashed lines represent $\pm 1\%$ error.

5 Concluding thoughts

For simplicity of illustration consider a storm that begins at time $t = 0$ with steady intensity and drop impact rate I. Suppose that we specify a desired length of resolution Y and an uncertainty $\sigma_{\bar{r}}$ in the calculated flux at x. The transverse length Y initially is larger than the desired resolution in order to satisfy the uncertainty criterion, then steadily decreases up to time $t = T$ coinciding with the desired resolution. In this scenario the distribution $f_r(r)$ is populated by an increasing number of particles to time $t = T$. Then, for $t > T$ the uncertainty criterion is satisfied by particles that crossed x during the preceding interval from $t - T$ to t. That is, the distribution $f_r(r)$ is continuously populated by the same number of particles, albeit a different set of particles from one instant to the next, in order to satisfy the uncertainty criterion. In this sense the calculated flux at time t is a time moving average. Alternatively, for a specified, fixed resolution Y throughout, the uncertainty $\sigma_{\bar{r}}$ initially is large then steadily decreases with time.

With unsteady rainfall during a storm, drop impacts are an inhomogeneous Poisson process

in time and the particle entrainment rate E_n is unsteady. This means that time averaging is not as straightforward as that suggested above. For a specified uncertainty the resolution of the calculated flux varies during a storm. This is the topic of a separate essay.

We must acknowledge that the actual uncertainty is larger than that defined by $\sigma_{\overline{r}}$. This is due to the ensemble variance associated with a specified Poisson impact rate I combined with the randomness of the number of entrained particles per drop impact (Appendix B). For the order-of-magnitude calculations above we have used only the expected rate I and the expected number $n_{\rm d}$.

In fluid mechanics and granular gas theory, continuum versus rarefied conditions are defined in terms of the Knudsen number, the ratio of the particle mean free path to a characteristic length scale. For rain splash transport the idea of a Knudsen number to define continuum conditions must be replaced with specification of the time averaging and spatial resolution involved in order to define a quasi-continuum-like behavior. Specifically, we can divide the net number $n(T)$ by Y to define the "local" particle flux as in (6). But it is important to recognize that this is not the flux at a precise Eulerian position as we normally envision for a continuum fluid. Rather, this time-averaged flux is only resolved at the scale Y.

Rain splash transport is a noise driven process. As such it is possible to conceptualize the flux q_x as a continuum-like ensemble expectation involving the expected quantities I, $n_{\rm d}$ and μ_r. This represents the imagined "climate" of the process, whereas fluctuations about the ensemble expectation in any realization represent its "weather" (Furbish and Doane, 2021).

A Particle transport

Let $f_r(r)$ denote the ensemble distribution of particle displacements r measured parallel to x about a drop impact. This distribution has mean μ_r and variance σ_r^2. Using elements of the analyses of Furbish and Haff (2010) and Furbish and Roering (2013), this distribution can be separated into two parts, one associated with negative displacements and the other with positive displacements. These are denoted as $f^*_{r-}(r)$ and $f^*_{r+}(r)$. The proportions of $f_r(r)$ represented by each are

$$p_- = \int_{-\infty}^{0} f_r(r)\,{\rm d}r \quad \text{and} \tag{10}$$

$$p_+ = \int_{0}^{\infty} f_r(r)\,{\rm d}r\,. \tag{11}$$

Note that p_- coincides with the probability that an entrained particle moves in a negative direction and p_+ is the probability that it moves in a positive direction. The normalized distributions, $f_{r-}(r)$ and $f_{r+}(r)$, are then given by

$$f_{r-}(r) = \frac{1}{p_-} f^*_{r-}(r) \quad \text{and} \tag{12}$$

$$f_{r+}(r) = \frac{1}{p_+} f^*_{r-}(r) \tag{13}$$

with means μ_{r_-} and μ_{r+}. The mean μ_r is recovered as

$$\mu_r = p_-\mu_{r-} + p_+\mu_{r+}\,, \tag{14}$$

which essentially is a weighted average.

Consider positive displacements. Let $F_{r+}(r)$ denote the cumulative distribution function so that $R_{r+}(r) = 1 - F_{r+}(r)$ denotes the exceedance probability function. If $E_n = In_{\rm d}$ denotes the expected steady, uniform entrainment rate, then the number of particles entrained within the area $Y{\rm d}x$ during the small interval ${\rm d}t$ is $YIn_{\rm d}{\rm d}x{\rm d}t$. Neglecting travel times, the number of particles entrained within $Y{\rm d}x$ at $x' \le x$ that move downslope of x during ${\rm d}t$ is $p_+YIn_{\rm d}R_{r+}(x - x'){\rm d}x{\rm d}t$. The total number that moves downslope of x during ${\rm d}t$ is

$$n_+(x;{\rm d}t) = p_+YIn_{\rm d}\int_{-\infty}^{x} R_{r+}(x-x')\,{\rm d}x'{\rm d}t\,, \tag{15}$$

and the total number moving past x during the interval T is

$$n_+(T) = p_+YIn_{\rm d}\int_{0}^{T}\int_{-\infty}^{0} R_{r+}(x-x')\,{\rm d}x'{\rm d}t\,. \tag{16}$$

With $r = x - x'$ a change of variables gives

$$n_+(T) = p_+ Y I n_\mathrm{d} \int_0^T \int_0^\infty R_{r+}(r)\,\mathrm{d}r\mathrm{d}t\,. \quad (17)$$

Evaluating the integrals then gives

$$n_+(T) = p_+ Y I n_\mathrm{d} \mu_{r+} T\,. \quad (18)$$

A similar development for negative particles displacements leads to

$$n_-(T) = p_- Y I n_\mathrm{d} \mu_{r-} T\,. \quad (19)$$

The sum of (18) and (19) gives the net number of particles crossing x during T. Namely,

$$n(T) = Y I n_\mathrm{d} (p_- \mu_{r-} + p_+ \mu_{r+}) T\,. \quad (20)$$

According to (14) the parenthetical part of (20) is equal to μ_r, so this is equivalent to (4) in the main text.

B Uncertainty in net particle number

There is uncertainty in the net number of particles $n(T)$ due to uncertainty in the number of drop impacts and the number of entrained particles per impact. We rewrite (18) and (19) as

$$n_+ = A n_\mathrm{d} \quad \text{and} \quad n_- = B n_\mathrm{d} \quad (21)$$

where $A = p_+ Y I \mu_{r+} T$ and $B = p_- Y I \mu_{r-} T$. Let σ_A^2 and σ_B^2 denote the variances associated with the expected values A and B and let $\sigma_{n_\mathrm{d}}^2$ denote the variance associated with n_d. Assuming the number of entrained particles per impact is uncorrelated with the number of drop impacts, then the variance $\sigma_{n_+}^2$ of n_+ is

$$\sigma_{n_+}^2 = A^2 n_\mathrm{d}^2 \left[\left(\frac{\sigma_A}{A} \right)^2 + \left(\frac{\sigma_{n_\mathrm{d}}}{n_\mathrm{d}} \right)^2 \right], \quad (22)$$

and the variance $\sigma_{n_-}^2$ of n_- is

$$\sigma_{n_-}^2 = B^2 n_\mathrm{d}^2 \left[\left(\frac{\sigma_B}{B} \right)^2 + \left(\frac{\sigma_{n_\mathrm{d}}}{n_\mathrm{d}} \right)^2 \right]. \quad (23)$$

The variance of the sum $n = n_+ + n_-$ is then

$$\sigma_n^2 = \sigma_{n_+}^2 + \sigma_{n_-}^2 + 2\sigma_{n_\pm}^2\,, \quad (24)$$

with covariance $\sigma_{n_\pm}^2$.

C Asymmetric Laplace distribution

We do not need to directly use the asymmetrical Laplace distribution. Nonetheless, for completeness and to show consistency with the analysis, here we describe this distribution.

The asymmetric Laplace distribution centered on $r = 0$ is

$$f_r(r;\lambda,\kappa) = \frac{\lambda}{\kappa + 1/\kappa} \begin{cases} e^{\lambda r/\kappa} & r < 0 \\ e^{-\lambda\kappa r} & r \geq 0\,, \end{cases} \quad (25)$$

with mean $\mu_r = (1-\kappa^2)/\lambda\kappa$ and variance $\sigma_r^2 = (1+\kappa^4)/\lambda^2\kappa^2$. Here $\lambda > 0$ is a scale parameter and $\kappa > 0$ is an asymmetry parameter. When $\kappa = 1$ this becomes the symmetric Laplace distribution. The proportion of the distribution representing negative displacements is $p_- = \kappa^2/(1+\kappa^2)$ so the proportion representing positive displacements is $p_+ = 1 - \kappa^2/(1+\kappa^2) = 1/(1+\kappa^2)$.

The normalized distribution of positive displacements is

$$f_{r_+}(r) = \lambda\kappa e^{-\lambda\kappa r} \qquad r \geq 0 \quad (26)$$

with mean $\mu_{r_+} = 1/\lambda\kappa$ and variance $\sigma_{r_+}^2 = 1/\lambda^2\kappa^2$. The normalized distribution of negative displacements is

$$f_{r_-}(r) = \frac{\lambda}{\kappa} e^{\lambda r/\kappa} \qquad r < 0 \quad (27)$$

with mean $\mu_{r_-} = -\kappa/\lambda$ and variance $\sigma_{r_+}^2 = \kappa^2/\lambda^2$. The mean displacement recovered by (14) is consistent with that stated above. Note that if the asymmetry parameter κ is not significantly different from one, then the probability $p_- \approx p_+$, which we use in the next appendix.

D Convergence

Of interest is the time T required to populate the distribution $f_r(r)$ such that it converges to a smooth form, implying that estimates of the moments μ_r, σ_r^2, μ_{r+} and μ_{r-} converge to their parametric values. This involves estimating the total number N of particles entrained in relation

T for a specified error $\sigma_{\overline{r}}$ of the estimate $\overline{r}$ of the mean μ_r. Here we are concerned with order-of-magnitude calculations, so we only work with expected quantities, acknowledging the additional uncertainty as described in Appendix B.

The total expected number is given by

$$N(T) = n_-(T) + n_+(T)$$

$$= YIn_{\mathrm{d}}(p_-|\mu_{r-}| + p_+\mu_{r+})T\,. \qquad (28)$$

So long as the distribution $f_r(r)$ is not strongly asymmetrical this can be approximated as

$$N(T) \approx YIn_{\mathrm{d}}\mu_{r+}T\,. \qquad (29)$$

Here we are assuming that μ_{r-} and μ_r converge at least as fast as μ_{r+} to their parametric values with increasing N. The central limit theorem then looks like

$$\sigma_{\overline{r}}^2 = \frac{\sigma_r^2}{YIn_{\mathrm{d}}\mu_{r+}T} \qquad (30)$$

This represents uncertainty of the ensemble. That is, it represents the uncertainty in the estimate of the mean displacement μ_r, and thus the flux q_x, associated with a great number (ensemble) of realizations, each subjected to the same physics as described by the impact rate I, the expected number of entrained particles per drop n_{d} and the mean displacement μ_{r+} for given transverse length Y and time T. Here we are assuming that the accumulation of particle numbers is a noisy process without temporal correlation beyond the particle ballistic time scale, in which case the averaging time T gives a quasi-random sample of size N.

Acknowledgments. We appreciate continuing discussions with Tom Dunne and Peter Haff.

References

[1] Dunne, T., Malmon, D. V., and Mudd, S. M. (2010) A rain splash transport equation assimilating field and laboratory measurements, *Journal of Geophysical Research – Earth Surface*, 115, F01001, doi: 10.1029/2009JF00130.

[2] Dunne, T., Malmon, D. V., and Dunne, K. B. J. (2016) Limits on the morphogenetic role of rain splash transport in hillslope evolution, *Journal of Geophysical Research – Earth Surface*, 121, doi: 10.1002/2015JF00373.

[3] Fick, A. (1855) Über diffusion, *Annual Review of Physical Chemistry*, 94, 59–86.

[4] Furbish, D. J., Fathel, S. L., Schmeeckle, M. W., Jerolmack, D. J., and Schumer, R. (2017) The elements and richness of particle diffusion during sediment transport at small timescales, *Earth Surface Processes and Landforms*, 42, 214–237, https://doi.org/10.1002/esp.4084.

[5] Furbish, D. J., Childs, E. M., Haff, P. K., and Schmeeckle, M. W. (2009) Rain splash of soil grains as a stochastic advection-dispersion process, with implications for desert plant-soil interactions and land-surface evolution, *Journal of Geophysical Research – Earth Surface*, 114, F00A03, doi: 10.1029/2009JF001265.

[6] Furbish, D. J. and Doane, T. H. (2021) Rarefied particle motions on hillslopes – Part 4: Philosophy, *Earth Surface Dynamics*, 9, 629–664, https://doi.org/10.5194/esurf-9-629-2021.

[7] Furbish, D. J. and Haff, P. K. (2010) From divots to swales: Hillslope sediment transport across divers length scales, *Journal of Geophysical Research – Earth Surface*, 115, F03001, doi: 10.1029/2009JF001576.

[8] Furbish, D. J., Hamner, K. K., Schmeeckle, M., Borosund, M. N., and Mudd, S. M. (2007) Rain splash of dry sand revealed by high-speed imaging and sticky paper splash targets, *Journal of Geophysical Research – Earth Surface*, 112, F01001, doi: 10.1029/2006JF000498.

[9] Furbish, D. J. and Roering, J. J. (2013) Sediment disentrainment and the concept of local versus nonlocal transport on hillslopes, *Journal of Geophysical Research – Earth Surface*, 118, 1–16, doi: 10.1002/jgrf.20071.

[10] Smith, J. A., Hui, E., Steiner, M., Baeck, M. L., Krajewski, W. F., and Ntelekos, A. A. (2009) Variability of rainfall rate and raindrop size distributions in heavy rain, *Water Resources Research*, 45, W04430.